

# Seismic Assessment of Typical 1970s Tall Steel Moment Frame Buildings in Downtown San Francisco

**Ibrahim Almufti, Carlos Molina Hutt, Michael Willford**  
*Arup, USA*

**Gregory Deierlein**  
*Stanford University, USA*



## SUMMARY:

An inventory of the existing tall building stock in San Francisco revealed that most tall buildings in the city were built in the 1970s and 1980s and adopted a steel Special Moment Resisting Frame (SMRF) structural system. In order to assess likely performance to current standards an archetypical 40-story steel SMRF building design was developed to represent the existing tall building stock. The building was designed per the 1973 Uniform Building Code (UBC 73), supplemented by the 1973 SEAOC Blue Book recommendations (SEAOC 1973), and employed connection details characteristic of the time.

Nonlinear response history analyses were carried out in LS-DYNA (LSTC) with ground motions representative of the Maximum Considered Earthquake (MCE) hazard level defined in current building codes, which for San Francisco is near a 1000 year return period due to the deterministic limit on the MCE. Under this level of shaking roughly 80 to 85% of the buildings are expected to sustain severe damage capable of causing loss of life and such that the structure may be at total economic loss. A small proportion of buildings may collapse.

*Keywords: Seismic, Retrofit, Tall Buildings, Steel Moment Frame, Fracture, LS-DYNA*

## 1. INTRODUCTION

San Francisco may be one of the most seismically vulnerable cities in the world due to its proximity to major active faults and its large number of older buildings. Until very recently, tall buildings in San Francisco were designed using only conventional building codes, which follow a prescriptive force-based approach based on the first mode translational response of the structure. Many researchers and engineers have raised concerns that the prescriptive approach of building codes is not suitable for tall buildings, which have significant responses in higher modes. Recognizing these shortcomings, several jurisdictions including Los Angeles (LATBSDC 2008) and San Francisco (SF AB-083 2003) have implemented guidelines which adopt a performance-based approach for new design. In light of these concerns and the potentially disproportionate consequences of tall building collapse in an urban environment, we intend to determine seismic collapse risk of the existing tall building stock in San Francisco by means of a modern performance-based assessment. This paper presents the findings of our initial intensity-based performance assessment representative of MCE-level shaking.

An inventory of the existing tall building stock was carried out by the SEAONC (Structural Engineers Association of Northern California) Committee on Performance-Based Design of Tall Buildings. This committee identified more than 90 buildings of 20 stories or greater, most of which employed a steel moment frame lateral system. While many researchers have assessed the performance of existing steel moment frame buildings of 30 stories and shorter (Muto and Krishnan 2011, Gupta and Krawinkler 1999), little is known of the performance of taller buildings. Muto found that approximately 5% of tall steel buildings in the 10-30 story range in the Los Angeles area would collapse and 15% would sustain damage capable of causing death due to a M7.8 scenario on the San Andreas Fault -Great Southern California Shakeout Scenario (Muto and Krishnan 2011).

In order to assess the seismic performance of existing tall buildings in San Francisco, non-linear response history analyses of a representative 40-story building were carried out using the software package LS-DYNA (LSTC), which accounts for both nonlinear material and geometric effects. We used 40 ground motion pairs selected and scaled based on the Conditional Spectrum of the 5% probability of exceedance in 50 year hazard, which is approximately equivalent to the code level Maximum Considered Earthquake (MCE) defined in ASCE 7 over the period range of interest for tall structures. The analysis employs robust non-linear component models to represent fracture of the welds, flexibility of the panel zones, degradation of the plastic hinges, tensile and flexural capacity of the column splices and buckling of the columns.

## 2. INVENTORY OF EXISTING TALL BUILDING STOCK IN SAN FRANCISCO

In order to categorize the seismic risk to existing tall buildings in San Francisco, the first task was to develop a database of all buildings taller than 160 feet ( $\approx 49$  meters). This was done in collaboration with the SEAONC Committee on Performance Based Design of Tall Buildings. Building characteristics were tabulated by location, height, number of stories, year built, lateral system type, and whether the building had been retrofitted (although the latter was difficult to determine). Much of the initial information was obtained from [www.emporis.com](http://www.emporis.com). Approximately 240 buildings taller than 160 feet were identified. Figure 1 illustrates the number of tall buildings built each decade between 1900 and 2010 (left) and the lateral system type for tall buildings built between 1960 and 1990 (right).

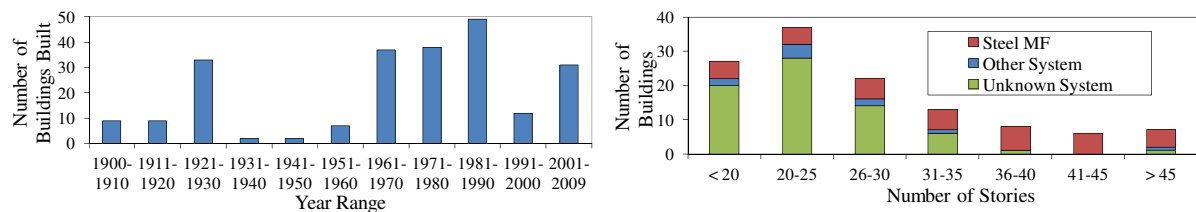


**Figure 1.** Number of tall buildings built in San Francisco per decade between 1900 and 2010 (left) and lateral system types for tall buildings built between 1960 and 1990 (right)

Information on the lateral system type was obtained by interviews with the Engineers of Record and a partial database gathered previously by the SEAONC committee. Information on the remaining buildings could only be obtained by viewing construction documents available at the building department. The lateral system type for approximately 80 out of the 240 buildings was identified. This data was de-aggregated to identify trends in order to select a ‘prototype’ building for this study. Figure 1 (right) shows the lateral system type for tall buildings built between 1960 and 1990. The sub-category ‘Other System’ means that the lateral system of the building is known and it is not a steel moment frame, while the sub-category ‘Unknown System’ is designated for all buildings for which the lateral system is unknown. From this data, it was determined that the steel moment frame system is the most prevalent type in pre-1990s construction for buildings greater than 35 stories in height.

A sidewalk survey was also conducted to visually inspect a random sample of 18 of the buildings identified. While several of the buildings were regular in plan (some with setbacks up the height), 6 of the 18 had no corner columns.

## 3. PROTOTYPE BUILDING

Based on the inventory presented in section 2, a 40-story steel SMRF was selected as a representative prototype building. The building is assumed regular in plan with corner columns; the implications of the absence of corner columns have not yet been investigated. The prototype building attempts to represent the state of design and construction practice from the mid 1970s to the mid 1980s. Based on

examination of existing building drawings, the following use and layout was assumed for our prototype building: 38 levels of office space; 2 levels (one at mid-height and one at the top) dedicated to mechanical equipment; 3 basement levels for parking; building enclosure composed of concrete panels and glass windows; floor system composed of concrete slab (3 inches or 76.3 mm) over metal deck (2.5 inches or 63.5 mm) supported by steel beams; steel grade of columns A572 and steel grade of beams A36. Typical story heights are 10 feet ( $\approx 3$  meters) for basement levels, 20 feet ( $\approx 6$  meters) at ground level (lobby) and 12.5 feet ( $\approx 3.75$  meters) for typical office levels. The overall height of the structure is 507.5 feet ( $\approx 153.75$  meters) above ground and 30 feet ( $\approx 9$  meters) below grade. The gravity loads, Superimposed Dead Load (SDL) and Live Load (LL), associated with the different spaces is summarized in Table 1 below

**Table 1.** Loading Assumptions

Use	SDL		LL		Use	SDL		LL	
	(psf)	(kPa)	(psf)	(kPa)		(psf)	(kPa)	(psf)	(kPa)
Parking	15	0.7	52	2.5	Mechanical	135	6.5	56	2.7
Lobby	90	4.3	100	4.8	Roof	85	4.1	32	1.5
Office	40	1.9	56	2.7	Façade	41	2.0	-	-

The prototype building was designed to the provisions of UBC 73 and the 1973 SEAOC Blue Book, which was commonly employed to supplement minimum design requirements. As illustrated in Figure 2, the prototype system consisted of a space frame with 20 to 40 feet spans ( $\approx 6$  to 12 meters) using wide flange beams, built up box columns, and welded beam-column connections. Typical member sizes and connection details were verified against construction drawings of existing buildings.

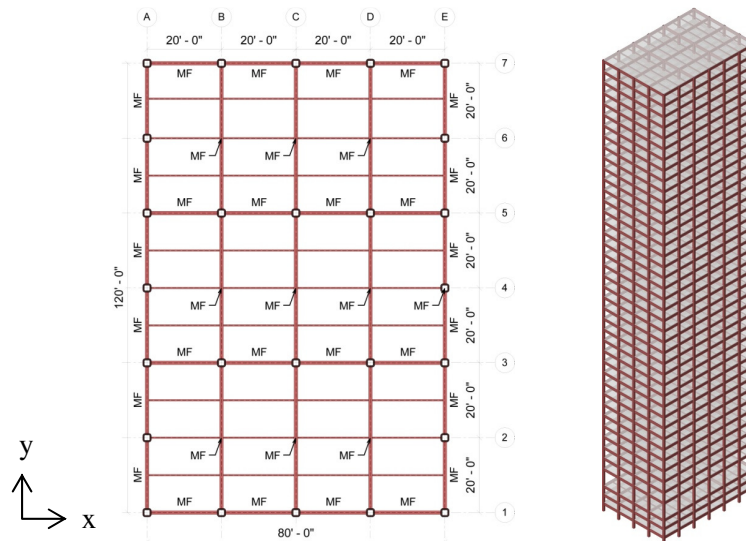


**Figure 2.** Prototype 40-story office building

Lateral wind forces generally govern over seismic for design, as illustrated in Figure 3. Per discussion with engineers practicing at this time, member sizes would have been sized for wind demand and detailed to provide a ductile response under seismic excitation. UBC 73 includes simple and concise prescriptive (equivalent static) strength design guidelines but does not specify drift limits. In the 1970s, design offices would have most likely implemented drift limits established by their firms practice or those obtained from the SEAOC Blue Book of the time. For this study, the drift limit recommendations from Appendix D of the SEAOC Blue Book are used, equal to 0.0025 for wind and 0.005 for seismic. The latter criterion is suggested for buildings taller than 13 stories. It is important to note that moment frame section sizes in the prototype building were governed by wind drift limits, resulting in low strength utilization ratios under code prescribed forces. Also worth noting is that such wind drift limits are similar to those currently used in the design of tall buildings.

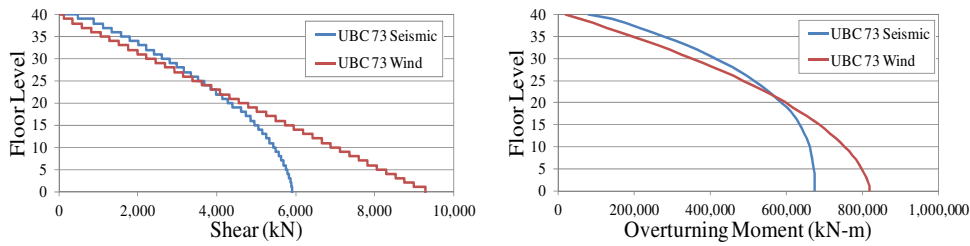


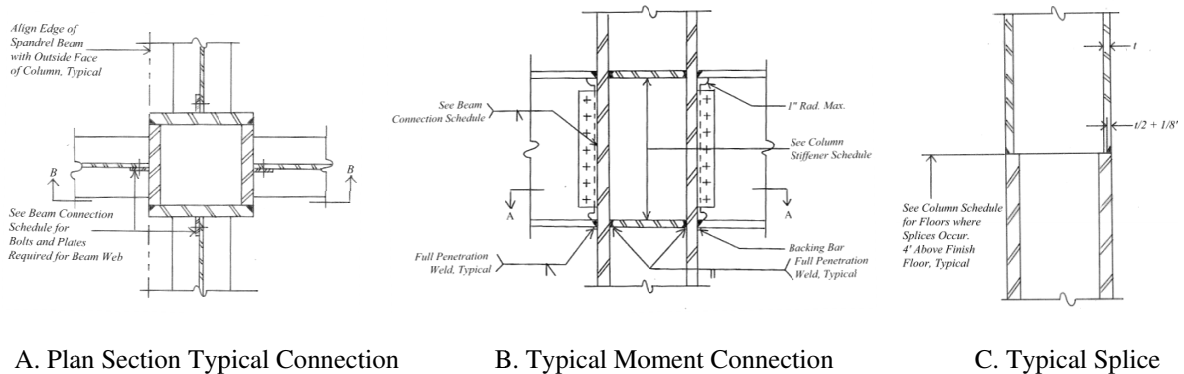
**Figure 3.** Cumulative wind and seismic base shears and overturning moments per UBC 73

Built-up box columns and wide flange beams were selected for the prototype building consistent with existing building drawings of this time. Table 2 below summarizes the column and beam section sizes used in our prototype building.

**Table 2.** Beam and Column Section Sizes per UBC 73 Design

Level Range	Wide Flange Beams			Box Columns		
	Ext. L=20'	Int. L=20'	Int. L=40'	Interior	Ext. Short (x)	Ext. Long (y)
Base to 10	W36x256	W36x282	W30x124	22x22x3.0x3.0	26x26x3.0x3.0	20x20x2.5x2.5
11 to 20	W33x169	W36x194	W27x84	20x20x2.0x2.0	26x26x2.5x2.5	20x20x2.0x2.0
21 to 30	W33x118	W33x169	W27x84	18x18x1.0x1.0	24x24x1.5x1.5	18x18x1.0x1.0
30 to Roof	W24x62	W27x84	W24x76	18x18x.75x.75	24x24x1.0x1.0	18x18x.75x.75

Typical details from drawings of existing buildings were reviewed to assess potential deficiencies. Figure 4 illustrates some typical connection details. The fracture prone pre-Northridge moment connections were very common, and the switch in the weld process that led to welds with very low toughness, as evidenced by fractures observed in the 1994 Northridge earthquake, took place in the mid 1960s (FEMA 352).



A. Plan Section Typical Connection      B. Typical Moment Connection      C. Typical Splice

**Figure 4.** Typical details observed in existing building drawings

It appears that the designs of the 1970's did not include consideration of panel zone flexibility or strong column-weak beam principles. Krawinkler's panel zone model was not developed until 1978 (ATC-72-1) and strong column weak beam requirements were not introduced in the UBC until 1988 (SAC/BD-00/25). However, considering the large column sizes required to satisfy axial and drift requirements in tall moment frames, weak panel zones or flexural strength of columns are not believed to be critical.

Column splices were typically located 4 feet ( $\approx 1.2$  meters) above the floor level approximately every three floors. Based on the typical splice connection details observed, if subject to tensile forces, these splices would only be able to carry half the capacity of the smallest section size being connected. Similarly, if subject to pure bending, these splices would have only been able to carry a fraction of the moment demand of the smallest column. Furthermore, experimental tests on heavy steel section welded splices had illustrated sudden failures with limited ductility (Bruneau and Mahin 1990). Based on this evidence column splice failures were considered as a significant factor in our assessment.

## 4. ANALYTICAL MODEL

This section outlines the modeling assumptions used in the non-linear response time history analyses in LS-DYNA (LSTC).

### 4.1. Component models

The component models to represent non-linear columns, beams, panel zones and splices are described below. Concrete slabs were modeled as elastic cracked concrete 2D shell elements to represent the flexible floor diaphragm.

#### 4.1.1 Columns

Columns were modeled as lumped plasticity beam elements with yield surfaces capable of capturing interaction between bi-axial bending moment and axial force. Buckling in compression is also captured. Degradation parameters for response under cyclic loads were calibrated based on experimental tests of tubular steel columns (Nakashima et al. 2007) following the guidelines for tubular hollow steel columns under varying levels of axial load (Lignos and Krawinkler 2010). Figure 5 below illustrates the component deterioration calibration results for two column samples with applied axial load to yield axial load ratios of 0.1 (left) and 0.3 (right) respectively.

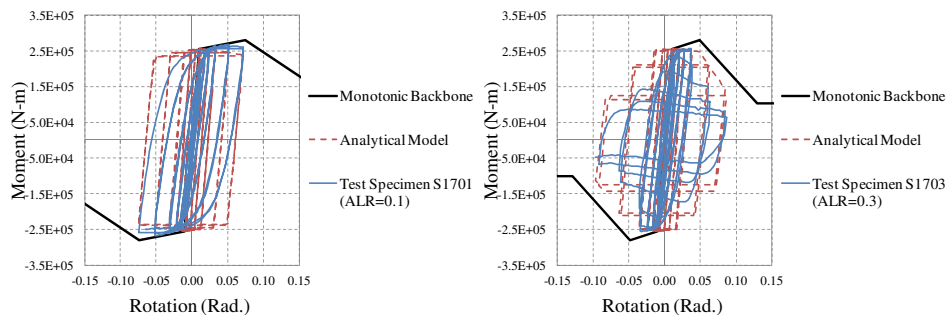


**Figure 5.** Calibration of column component deterioration under varying levels axial load

Typical axial load to axial capacity utilization ratios were tracked through a nonlinear response history analysis for a small sample of columns. It was determined that an applied load ratio of 0.3 was a good representation for our prototype building design and the intensity level under consideration.

#### 4.1.2 Beams

Beams that form part of the moment frames were modeled as lumped plasticity elements with implicit degradation in bending to capture random fracture at the connections. The random fracture model follows the methodology proposed by Maison and Bonowitz (1999), in which the plastic rotation at which fracture occurs is a random variable characterized by a truncated normal distribution following tests designed for typical pre-Northridge practice. Top and bottom capacities are modeled as a single random variable with a mean of 0.006 radians and a standard deviation of 0.004 radians. The truncated normal distribution and sample hysteretic behavior of beams with random fracture are shown in Figure 6.

The truncated tails at zero plastic rotation denote fracture prior to yield, which is supported by data from the SAC studies. In these cases, fracture is set to occur at 70% of the moment capacity of the beam. The residual moment capacity after fracture is set at 25% of the beam capacity.

For each of the analysis runs presented in this study, a different random fracture sample was obtained for each of the moment connections in the building model. Therefore, all analysis runs have a unique distribution of plastic rotation capacities throughout the structure. However, for any model, all samples of plastic rotation at fracture fit the distribution presented in Figure 6.



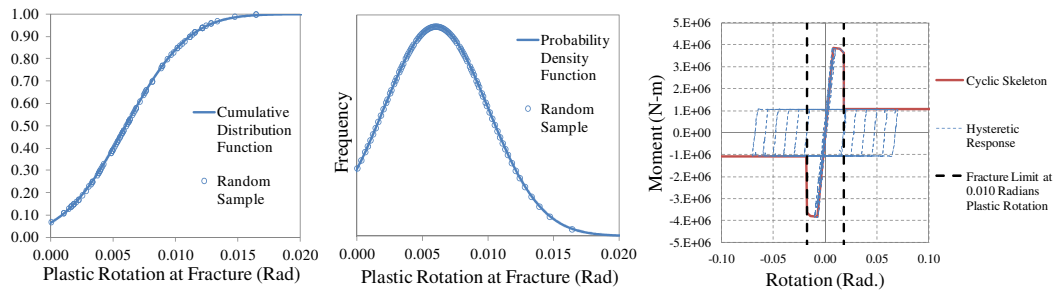


**Figure 6.** Probability distribution and sample hysteretic response for random fracture in connections

#### 4.1.3 Panel zones

Panel zones were modeled using the Krawinkler model as outlined in ATC-72-1 by the use of an assembly of rigid links and rotational springs that capture the tri-linear shear force-deformation relation. Since the prototype building model is three dimensional and columns are built-up box sections, the shear force-deformation relationship in each direction was assumed decoupled.

#### 4.1.4 Column splices

Column splices were modeled as non-linear springs capable of reaching their nominal capacity with a sudden brittle failure followed by 20% residual capacity when subject to axial tension and/or bending. Full column capacity was assumed in compression since this is achieved by direct bearing.

### 4.2 Loads, damping and boundary conditions

Analytical models were subject to the ground motions described in section 6 in conjunction with expected gravity loads associated with the seismic weight of the structure. Seismic weight was assumed to include selfweight, superimposed dead load and 25% of the unreduced live loads (PEER 2010). Since the hazard level under consideration corresponds to that of the code MCE, 2.5% damping was assumed in the analysis (PEER 2010). The damping model used in the analysis applies damping to deformation, excluding rigid body motion. The damping is adjusted based on tangent stiffness- which is believed appropriate for non-linear seismic analysis. A fixed base is assumed at foundation level and soil-structure interaction is not considered.

## 5. SEISMIC HAZARD

The majority of tall buildings in San Francisco are densely clustered in the downtown area, located approximately 15km from the two major faults in the Bay Area. The San Andreas fault is capable of producing M8.0 events while the Hayward fault is capable of producing M7.2 events. The study assumes Site Class D per ASCE 7, which is typical for downtown San Francisco sites.

### 5.1 Assessment of MCE

A site-specific Probabilistic Seismic Hazard Analysis (PSHA) for the 2% in 50 year hazard was carried out in EZ-FRISK using three NGA relationships (B&A 08, C&B 08 and C&Y 08). For sites in close proximity to faults in regions of high seismicity, the MCE is capped by a deterministic limit, defined as 150% of the largest median  $S_a$  geomean response (ASCE 7-05) or 84<sup>th</sup> percentile  $S_a$  maximum direction response (ASCE 7-10) computed at each period for all known faults in the region. In downtown San Francisco, the M8.0 scenario on the San Andreas fault governs the deterministic hazard at all periods. However, the default deterministic limit of chapter 21 of ASCE 7-05 and ASCE 7-10 ( $S_s = 1.5g$  and  $S_1 = 0.6g$  for bedrock and  $S_{MS} = 1.5g$  and  $S_{M1} = 0.9g$  for Site Class D) governs the code level MCE for San Francisco. Figure 7a compares all these 5% damped acceleration spectra.

At  $\bar{T} = 5$  seconds, the ASCE 7 MCE spectral acceleration is approximately 0.18g. De-aggregation of the MCE shows the mean causal magnitude is M7.72 on the San Andreas fault, the mean causal

distance (R) is 15.6km and the mean causal  $\epsilon$  is 0.99. The site-specific PSHA suggests that the true return period associated with the code level MCE at 5 seconds period is approximately 1000 years (5% probability of exceedance in 50 year hazard). Figure 7b shows that the 5% in 50 year hazard matches the code level MCE well for all periods between 2 and 8 seconds.

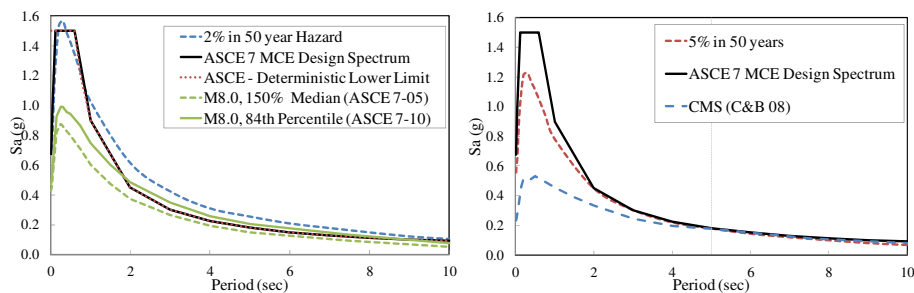


**Figure 7.** Code level MCE spectrum for Site Class D compared against 2% in 50 year PSHA and deterministic scenarios (left) and 5% in 50 year PSHA and CMS based on the C&B 08 NGA (right)

## 5.2 Development of Conditional Spectrum

Based on the above information, a Conditional Spectrum (CS) approach for a 5% in 50 year hazard, conditioned on the average fundamental period of the prototype building, was selected to carry out the intensity based assessment. The fundamental period was selected for conditioning because it provides a good estimate of the distribution of displacement demands (NIST GCR 11-917-15), appropriate for assessment of tall building performance. The Conditional Mean Spectrum (CMS) based on the C&B 08 NGA relationship, using M7.72 and R= 15.6km is compared in Figure 7b with the 5% in 50 year Uniform Hazard Spectrum (UHS) and the code level MCE spectrum. As expected, the CMS is close to the UHS spectrum for long periods, but significantly lower for periods shorter than 2 seconds.

## 6. GROUND MOTION SELECTION AND SCALING

### 6.1 Record sets selected

The response of the building was assessed using 40 pairs of seed ground motions, selected and linearly scaled from the NGA database available on the PEER website such that the geometric mean of the as-recorded motions matched the mean and conditional variability of the target CS. The selection and scaling was done automatically using the Matlab tools available from Professor Jack Baker's website [http://www.stanford.edu/~bakerjw/gm\\_selection.html](http://www.stanford.edu/~bakerjw/gm_selection.html). The geometric mean is deemed an appropriate target since it is unlikely that the maximum direction will align with the principal axes of the structure for all ground motions (Stewart et al. 2011). The number of ground motions selected was based on recommendations provided in NIST GCR 11-917-15 for intensity-based assessments. Figure 8 shows geometric mean response spectra of the 40 pairs plotted against the target CS.

### 6.2 Effect of velocity pulses

The current hazard assessment and ground motion selection, whilst consistent with current code spectra, does not explicitly account for velocity pulse like motions. Whilst 10 of the 40 motions selected did contain some form of velocity pulse, seven of which have a pulse period greater than 4 seconds, there was no quantitative basis for this. We have recently implemented the Shahi and Baker (2011) method for incorporating near-fault pulse effects into our *Oasys* SISMIC PSHA software. For downtown San Francisco, this statistical incorporation of pulse like motions increases the 5% in 50 year spectral acceleration at T = 5 seconds by approximately 65%, and indicates that 36 of the 40

motions should in fact contain pulses. This indicates that the structural responses described in section 7 might be significantly underestimated.

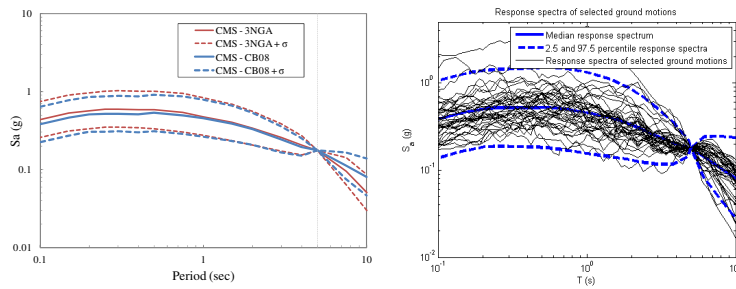


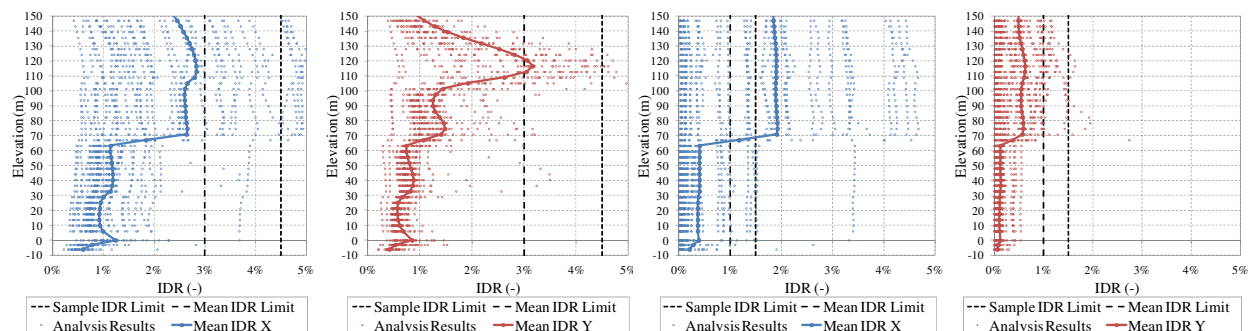
**Figure 8.** CS computed using 3NGA and C&B 08 only (left) and ground motions scaled to target CS (right)

## 7. BUILDING PERFORMANCE PREDICTIONS

### 7.1 Interstory Drift Ratios (IDRs)

PEER (2010) proposes that for MCE level shaking, mean IDRs should be limited to 3% and the maximum transient IDRs from the suite of analyses to 4.5%. This is on the basis that structural components with a proper yielding mechanism will perform well and non-structural components properly attached to the structure will not pose a life safety hazard. Residual drift limits are also important in determining the required downtime associated with excessive post-earthquake deformations, which could lead to condemnation as well as hazard to surrounding structures in the event of aftershocks. The corresponding PEER recommendations for MCE, limits the mean residual IDRs to 1% and the maximum residual IDRs from the suite of analyses to 1.5%. However, significant non-structural damage and extended downtime or even building condemnation would be expected if mean residual drifts exceed 0.5%.

Predicted transient and residual IDRs are shown in Figure 9. It can be observed that the peak interstory drifts tend to occur near mid-height and the top of the structure. This may be attributable to the governing structural design criteria per UBC 73 being drift control under wind forces, not seismic.



a) Peak transient IDRs in x and y

b) Peak residual IDRs in x and y

**Figure 9.** Transient and residual IDRs against height

The overall distributions of peak transient and residual IDRs are shown in Figure 10. Rather than only evaluating IDRs against the limits provided by PEER (2010), which are intended to ensure code-level performance, peak transient and residual IDRs were also classified into damage state IDR categories as described in ATC-58-1. Results illustrate 80 to 85% chance of Damage State 3 (DS3) or worse. DS3 is characterized by the requirement of major structural realignment to restore safety margin for lateral stability; however, the required realignment



and repair of the structure may not be economically and practically feasible (i.e., the structure might be at total economic loss) as described in ATC-58-1.

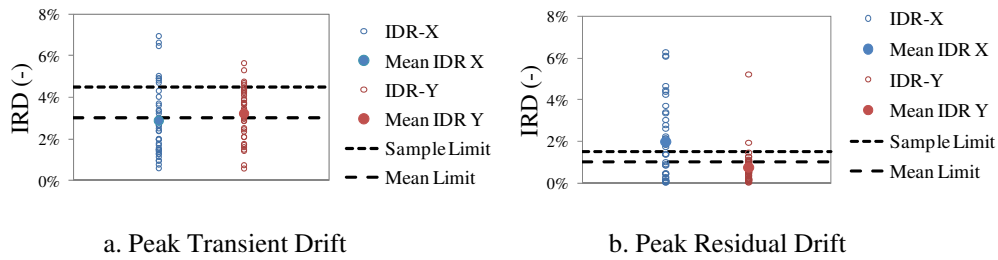


**Figure 10.** Peak transient and residual drifts

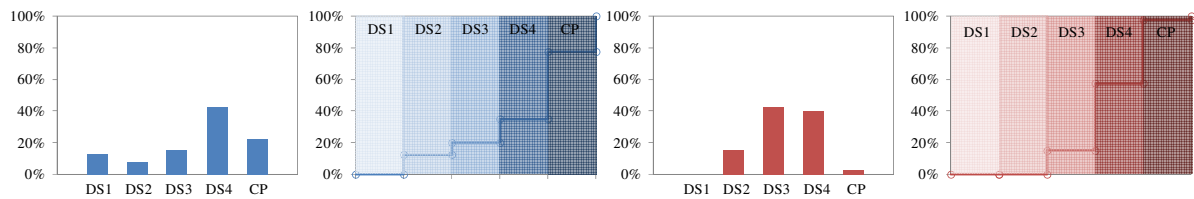


**Figure 11.** Damage state (DS) and Collapse (CP) classification per transient (left) and residual (right) IDRs

## 7.2 Performance of structural components

On average, 34% of moment connections yielded and 15% of connections fractured, which would compromise the strength and stiffness of the structure in the event of aftershocks and later earthquakes until retrofit measures are adopted. As anticipated, typically the panel zones in the large built up box columns did not suffer significant levels of deformation due to their inherent strength and stiffness. Local tension demands in column splices were typically below nominal capacities and brittle fracture leading to collapse was only observed in one of the analysis runs. In this case splice fracture occurred near mid-height of the structure and led to collapse. Columns often reached their nominal capacities in bending and compression, but did not undergo extensive deterioration (because they are so stocky) and hence do not compromise the overall stability of the structure.

## 8. POTENTIAL RETROFITS

In order to enhance the seismic performance of typical 1970s tall steel moment frame buildings, a reduction in transient and residual deformations is required. This objective can be achieved by adding stiffness, damping or a combination of these to the structure. Based on the response of the structural components, direct retrofit of the deficiencies identified in this study will not suffice to significantly enhance seismic performance. Specific retrofit measures will be explored in future studies.

## 9. CONCLUSIONS

The performance of tall 1970s steel moment frame buildings in downtown San Francisco under earthquake shaking levels consistent with the code MCE are expected to produce an 80 to 85% chance of damage that will require major structural realignment such that the required realignment and repair of the structure may not be economically and practically feasible. Significant structural and non-structural damage is expected. Damage capable of producing loss of life, significant losses attributed to structural and non-structural damage, downtime and potential building condemnation are anticipated. Since drift limits largely controlled member sizes, buildings which followed less stringent limits or which did not follow any limits (not required by the code of the time) are expected to undergo larger deformations and present a greater risk of severe damage or collapse.

An important consideration is that incorporation of recent research into the presence of velocity pulses in ground motions associated with large events would significantly increase the degree of damage and number of collapses predicted.

#### **ACKNOWLEDGEMENT**

SEAONC Tall Buildings Committee, David Leung, Janice Mochizuki, Bryce Tanner, Jason Krolicki, Ramin Motamed, Jack Backer, Damian Grant, Dimitrios Lignos, Tiziana Rossetto, David Scott and Rafael Sabelli.

#### **REFERENCES**

- Applied Technology Council. (2012). Seismic Performance Assessment of Buildings. ATC-58-1 100% Draft.
- Baker J. (2011). Conditional Mean Spectrum: Tool for Ground-Motion Selection. *Journal of Structural Engineering*, **Vol. 137**, **No. 3**.
- Baker J., Jayaram N. (2008). Correlations of Spectral Acceleration Values from NGA Ground Motion Models. *Earthquake Spectra*, **Vol. 23**, **No. 1**, pages 299-317.
- Bruneau M., Mahin, S. (1990). Ultimate Behavior of Heavy Steel Section Welded Splices and Design Implications. *Journal of Structural Engineering*, **Vol. 116**, **No. 8**.
- FEMA. (2000). Program to Reduce the Earthquake Hazards of Steel Moment-Frame Structures: Recommended Postearthquake Evaluation and Repair Criteria for Welded Steel Moment-Frame Buildings. FEMA 352.
- Gupta A., Krawinkler H. (1999). Seismic Demands for Performance Evaluation of Steel Moment Resisting Frame Structures. Dept. of Civil and Environmental Engineering, Stanford University. Report No. 132.
- International Conference of Building Officials. (1973). Uniform Building Code 1973 Edition.
- LATBSDC. (2008). An Alternative Procedure for Seismic Analysis and Design of Tall Buildings Located in the Los Angeles Region.
- Lignos D., Krawinkler H. (2010). A Steel Database for Component Deterioration of Tubular Hollow Square Steel Columns Under Varying Axial Load for Collapse Assessment of Steel Structures under Earthquakes. Joint Conference Proceedings 7CUEE & 5ICEE.
- Maison F., Bonowitz D. (1999). How Safe Are Pre-Northridge WSMFs? A case Study of the SAC Los Angeles Nine-Story Building. *Earthquake Spectra*, **Vol. 15**, **No. 4**.
- Muto M., Krishnan, S. (2011). Hope for the Best, Prepare for the Worst: Response of Tall Steel Buildings to the ShakeOut Scenario Earthquake. *Earthquake Spectra*, **Vol. 27**, **No. 2**, pages 375-398.
- Nakashima M. et al. (2007). Test on Large Cyclic Deformation of Steel Tube Columns Having Fixed Column Bases. *Journal of Structural and Construction Engineering*, **Vol. 598**, pages 149-154.
- NEHRP Consultants Joint Venture. (2011). Selecting and Scaling of Earthquake Ground Motions for Performing Response-History Analyses. NIST GCR 11-917-15.
- PEER. (2010). Tall Buildings Initiative: Guidelines for Performance-Based Seismic Design of Tall Buildings. PEER Report No. 2010/05.
- PEER/ATC. (2010). Modeling and Acceptance Criteria for Seismic Design and Analysis of Tall Buildings. PEER/ATC-72-1.
- SAC Joint Venture. (2000). Performance Prediction and Evaluation of Steel Special Moment Frames for Seismic Loads. SAC Steel Project Report No. SAC/BD-00/25.
- SEAONC AB-083. (2007). Recommended Administrative Bulletin on the Seismic Design and Review of Tall Buildings Using Non-Prescriptive Procedures.
- SEAOC Seismology Committee. (1973) Recommended Lateral Force Requirements and Commentary.
- SEAONC Seismology Committee on Ground Motions. (2009). 2475-year Ground Motion? Not in Coastal California! *SEAONC News*, **Vol. LXIV**, **No. 8**.
- Shahi S., Baker J. (2011). An empirically calibrated framework for including the effects of near-fault directivity in probabilistic seismic hazard analysis. *Bulletin of the Seismological Society of America*, **Vol. 101**, **No. 2**, pages 742-755.
- Stewart J. et al. (2011). Representation of Bidirectional Ground Motions for Design Spectra in Building Codes. *Earthquake Spectra*, **Vol. 27**, **No. 3**, pages 927-937.